Journal of South American Earth Sciences 151 (2025) 105273

Contents lists available at ScienceDirect

Journal of South American Earth Sciences

journal homepage: www.elsevier.com/locate/jsames

New pterosaur fossils from the Early Cretaceous of Colombia

Edwin-Alberto Cadena [a,b,c,*], Dubban A. Atuesta-Ortiz [d], Jeffrey A. Wilson Mantilla [e,f]

[a] Facultad de Ciencias Naturales, Grupo de Investigación Paleontología Neotropical Tradicional y Molecular (PaleoNeo), Universidad del Rosario, Bogotá, 111221, Colombia
[b] Smithsonian Tropical Research Institute, Box 0843–03092, Balboa, Ancón, Panama
[c] Field Museum of Natural History, Chicago, IL, 60605, USA
[d] Servicio Geológico Colombiano, Bogotá, Colombia
[e] Museum of Paleontology, University of Michigan, 1105 N. University Avenue, Ann Arbor, MI, 48109-1085, USA
[f] Department of Earth & Environmental Sciences, University of Michigan, 1100 North University Avenue, Ann Arbor, MI 48109-1005, USA

A B S T R A C T

The fossil record of pterosaurs in northwestern Gondwana has been relatively scarce, with only two previous occurrences. This study presents new pterosaur findings from three sites in Colombia, including a new record of an *Anhanguera*-like specimen and other bones referrable to Anhangueria. The new material includes a distinctive partial lower jaw found in association with parts of a radius and a complete distal syncarpal. The lower jaw has a triangular glenoid fossa in dorsal view, a fossa depressoria with a bean-shaped outline, and a retroarticular process with a straight margin in lateral or medial views. The new fossils extend the record of *Anhanguera*-like pterosaurs into the earliest part of the Cretaceous and expand our knowledge of the vertebrate fossil record of lower latitudes.

1. Introduction

The fossil record of pterosaurs from northern South America is poorly sampled thus far, with just two occurrences, both from Early Cretaceous-aged horizons. The first, from the Aptian Apón Formation of Venezuela, is a nearly complete, isolated scapulocoracoid whose size and proportions match those of anhanguerids (Kellner and Moody, 2003). The second, from the Valanginian Rosa Blanca Formation of Colombia, includes a partial radius with ctenochasmatoid or azhdarchoid affinities and a lower jaw resembling ornithocheiroids (Cadena et al., 2020). However, the incompleteness of these remains precludes further systematic analysis, leaving unresolved the affinities of the pterosaurs from this region.

Here, we describe new and better-preserved pterosaur remains from two localities in the Valanginian Rosa Blanca Formation of Zapatoca, Santander, Colombia (Fig. 1). Although these remains are insufficient to justify naming a new species, they support the hypothesis forwarded by Cadena et al. (2020) that the pterosaurs from this formation resemble *Anhanguera* (Campos and Kellner, 1985) from the Early Cretaceous of Brazil. Additionally, we expand the fossil record of pterosaurs in Colombia by reporting and describing the first Barremian record from the La Paja Formation in Villanueva, Santander (Fig. 1). These specimens contribute to the growing knowledge of pterosaurs from low latitudes in the Americas.

2. Material and methods

2.1. Fossil preparation and study

Rock matrix was removed from some specimens using dental picks. One specimen required preparation from an air scribe and sulfamic acid (H_3NSO_3) at the Centro de Investigaciones Paleontológicas in Villa de Leyva, Colombia.

The fossils were measured using a caliper, and they were photographed and examined with a Nikon Eclipse SMZ1270 stereomicroscope at the laboratory of the Traditional and Molecular Neotropical Paleontology Group (PaleoNeo) at the Universidad del Rosario.

In order to infer growth patterns of some of the specimens, thin sections from long bone fragments were prepared at the Mineral Lab company, Bogotá, Colombia (see below, "Bone Histology"). The thin sections were studied and photographed using polarized-light and Blue Color Balancing Filter (DLF) on a Leica DM750P microscope at the PaleoNeo lab, Universidad del Rosario.

* Corresponding author. Facultad de Ciencias Naturales, Grupo de Investigación Paleontología Neotropical Tradicional y Molecular (PaleoNeo), Universidad del Rosario, Bogotá, 111221, Colombia.
E-mail address: edwin.cadena@urosario.edu.co (E.-A. Cadena).

https://doi.org/10.1016/j.jsames.2024.105273
Received 30 September 2024; Received in revised form 19 November 2024; Accepted 20 November 2024
Available online 22 November 2024

2.2. Institutional abbreviation

UR-CP, paleontological collection, Facultad de Ciencias Naturales, Universidad del Rosario, Bogotá, Colombia.

3. Systematic paleontology

PTEROSAURIA, Kaup (1834).
PTERODACTYLOIDEA, Plieninger (1901).
ORNITHOCHEIROIDEA, Seeley (1870).
ANHANGUERIA sensu Rodrigues and Kellner (2013).
(Figs. 2–4A–H).

Referred material—Specimen UR-CP-0233 includes the posterior portions of the right and left rami of the mandible, the distal end of a ceratobranchial, proximal and distal portions of a left radius, and a complete left distal syncarpal.

Locality, Horizon, and Age— Specimen UR-CP-0233 is from El Sapo South locality, which is located approximately 3 km east-northeast of Zapatoca, in the Department of Santander, Colombia (6° 50′ 6′′ N, 73° 14′ 29′′ W). The bones were found associated within an area of approximately 1.5 m^2 at the top of a hard biomicrite limestone, which corresponds to layer Q^{IV} of the Carrizal Member, Rosa Blanca Formation (Etayo-Serna and Guzmán-Ospitia, 2019). The Carrizal Member of the Rosa Blanca Formation is within the upper Valanginian stage of the Lower Cretaceous based on ammonoid biostratigraphy zonation (Etayo-Serna and Guzmán-Ospitia, 2019; Szives et al., 2024).

Remarks— Specimen UR-CP-0233 shares with *Anhanguera* the rectangular shape in medial or lateral views of the mid-posterior regions of the rami and a retroarticular process moderately developed posterior to the glenoid fossa. It differs from *Anhanguera* and other pterosaurs in having triangular shape of the glenoid fossa in dorsal view, a fossa depressoria exhibiting a bean-shaped outline, and a retroarticular process that exhibits a straight margin in lateral or medial views.

Description— Specimen UR-CP-0233 consists of the posterior

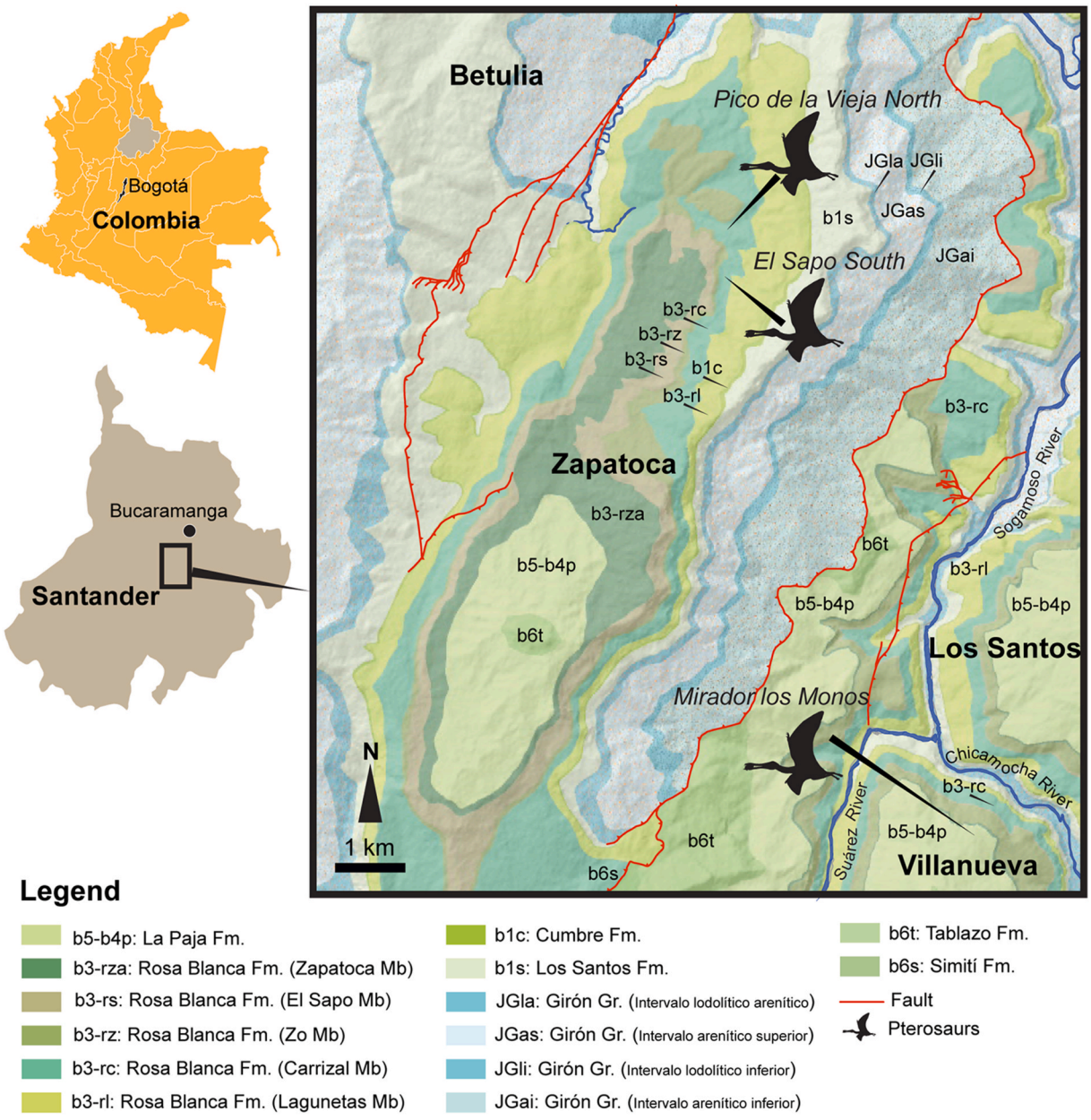

Fig. 1. Maps and localities in the Department of Santander, Colombia, where the fossil pterosaurs described herein were found, including two localities from Zapatoca (Pico de la Vieja North and El Sapo South) and one from Villanueva (Mirador los Monos).

portions of the right and left mandibular rami, and the distal tip of a ceratobranchial. All these elements were found associated, and some regions of the bones have been covered by a hard layer of hematite. The right mandibular ramus is more complete than is the left (Fig. 2A–G, J). In lateral view (Fig. 2A and B), its retroarticular process is high and short dorsoventrally, ending in a straight posterior margin. In lateral view, the sutural contact between the angular and the surangular is visible, as well as the contact between the prearticular and the surangular. Anterior to the tip of the prearticular there is a foramen. In medial view (Fig. 2C and D), the adductor fossa is well developed, and anteriorly projecting. It holds the foramen chorda tympani towards its posterior end. In dorsal view (Fig. 2E, F, J), the fossa depressoria is large and has a bean-shaped outline, and the glenoid fossa is deep, having a triangular shape.

The left mandibular ramus is less complete than the right (Fig. 2H

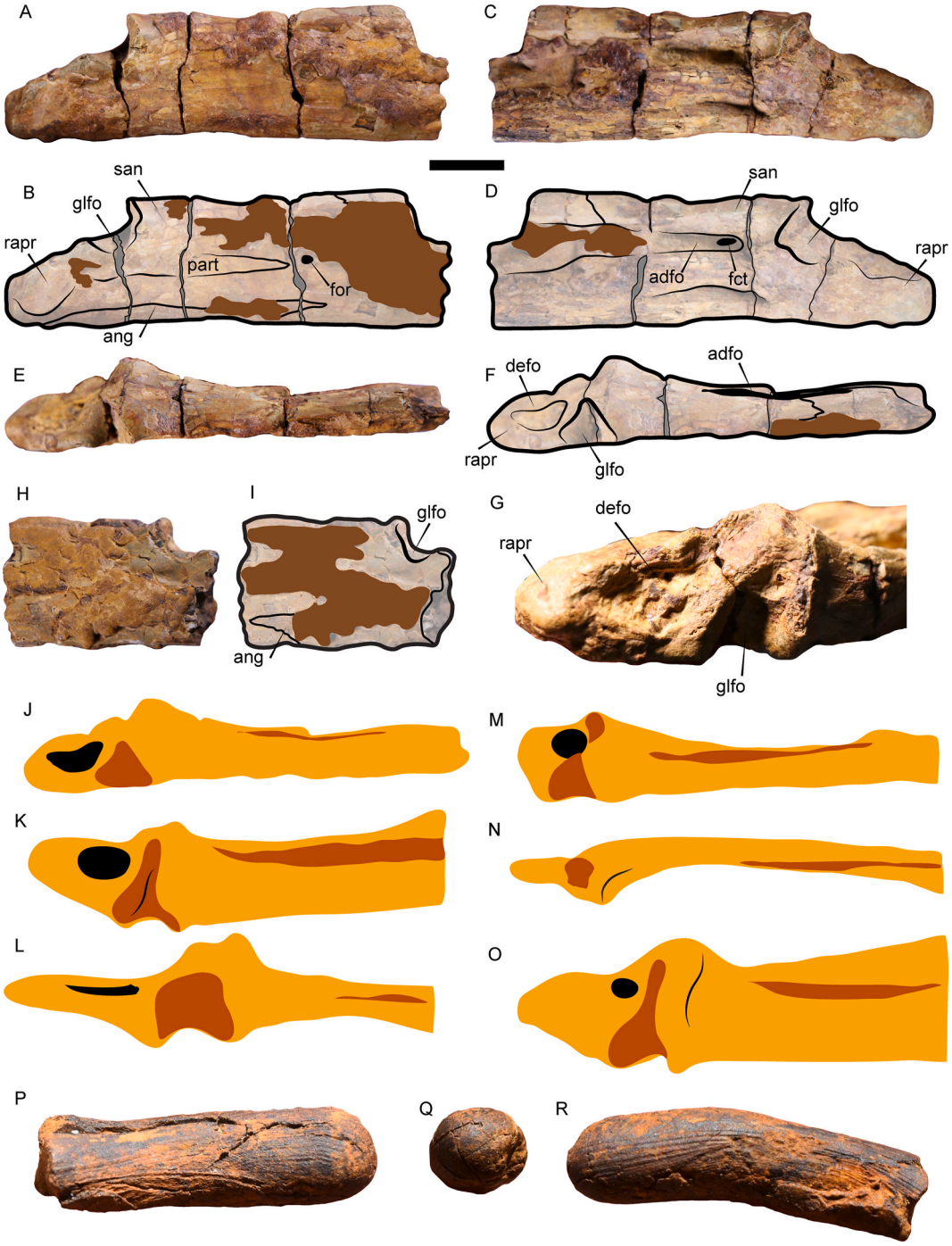

Fig. 2. Specimen UR-CP-0233, mandibular rami and ceratobranchial bones. **A–B**, right ramus in lateral view; **C–D**, right ramus in medial view; **E–G**, right ramus in dorsal view, including a close-up (G) of the posterior articular region; **H–I**, left ramus in lateral view; **J–O,** comparisons of the posterior articular right ramus of specimen UR-CP-0233 and several pterosaurs in dorsal view redrawn from Pêgas et al. (2021, Fig. 16), including: (J), cf. *Anhanguera*; (K) "*A. araripensis*"; (L), *Pteranodon* sp. YPM- 2410; (M), *Thalassodromeus sethi* holotype; (N), *Aymberedactylus cearensis* holotype; (O), *Pteranodon* sp. LACM- 51130; **P–R**, fragment of a ceratobranchial of specimen UR-CP-0233 in: (P), lateral view; (Q) posterior view; and (R), medial view. **Abbreviations**: **adfo**, adductor fossa; **ang**, angular bone; **defo**, fossa depressoria; **fct**, foramen chorda tympani; **for**, foramen; **glfo**, glenoid fossa; **part**, prearticular bone; **rapr**, retroarticular process; **san**, surangular bone. Scale bar equals 1 cm.

and I). It has the same deep and triangular shape of the glenoid fossa exhibited by the left ramus. Both the lateral and medial surfaces are still covered by a layer of hematite that is very difficult to remove, which leaves visible only the most anterior contact between the angular and the surangular. The retroarticular portion of the ramus is missing. A rod-like distal end of a ceratobranchial bone is also preserved, and fully replaced in hematite (Fig. 2P–R). The surface of the bone bears well-defined striations.

Specimen UR-CP-0233 also includes both proximal and distal portions of a left radius. For this and other wing elements, we follow other authors in orienting the wing in an outstretched position, such that anterior is towards its leading edge and posterior is towards its trailing edge (e.g., Andres and Langston, 2021; Rosenbach et al., 2024). The proximal portion of the left radius is nearly complete, lacking only its dorsal expansion and some of the cortical bone on its anterior face (Fig. 4A–D). The anterior and posterior surfaces of the proximal end are very smooth, and where this surface is broken away a very thin layer of cortical bone and highly pneumatic bone tissue are revealed (Fig. 4B and C). The shaft of the bone expands towards the distal end, but the characteristic dorsal expansion of the radius is not preserved. Its ventral side, however, preserves a rounded tubercle that extends beyond the edge of the proximal articular surface, which is shallow and dished (Fig. 4D). Much of its perimeter is bordered by a raised ridge of bone (ca. 0.8 mm thick). The proximal end flattens and tapers anteroposteriorly towards its preserved dorsal end.

The distal portion of the left radius preserves a small portion of the shaft and the entirety of the distal articular surface (Fig. 4E–H). The shaft is subrectangular in cross section, with its anteroposterior depth

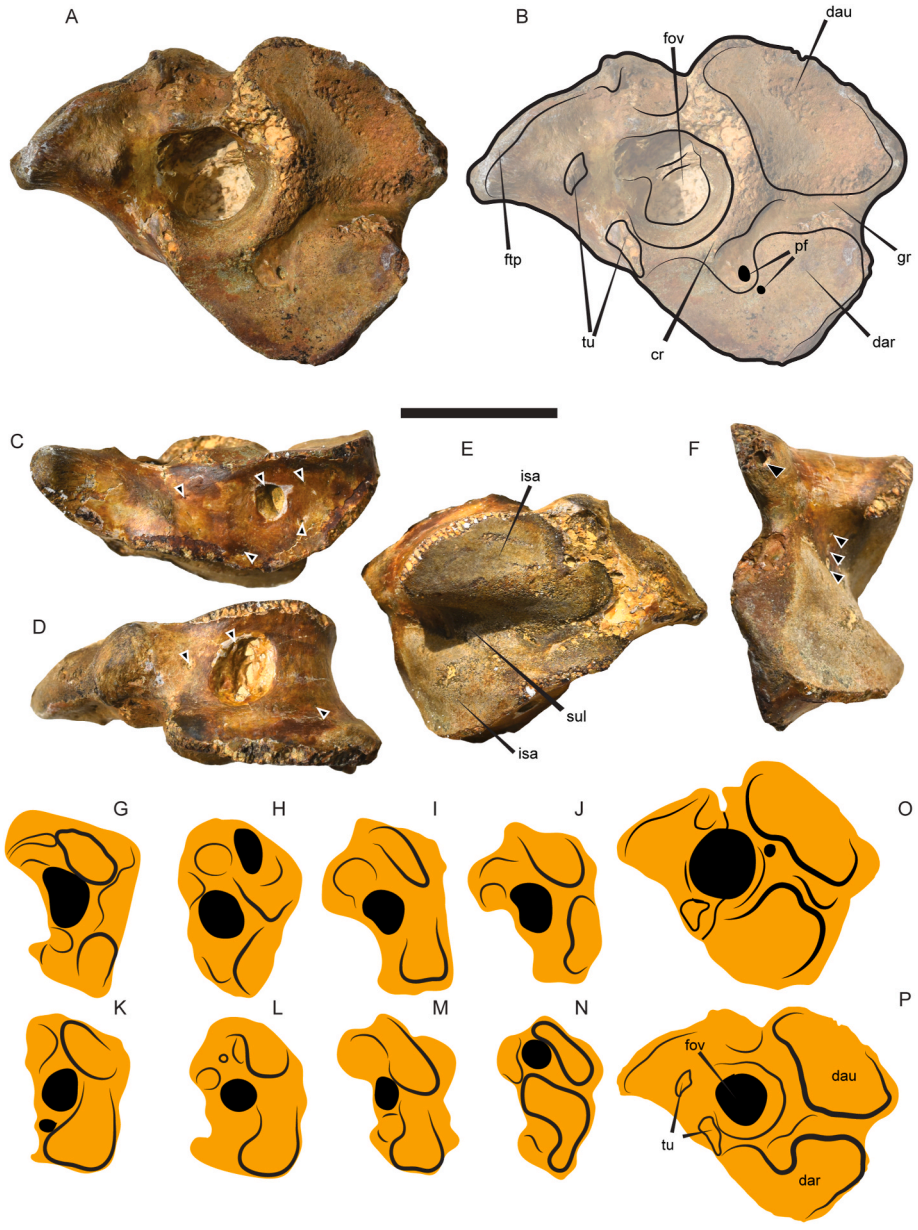

Fig. 3. Specimen UR-CP-0233, a complete left distal syncarpal. **A–B**, proximal view; **C**, anteroventral view; **D**, dorsal view; **E**, distal view; **F**, posterior view; **G–O,** comparisons of the left distal syncarpal of specimen UR-CP-0233 and some Cretaceous pterodactyloids redrawn from Rigal et al. (2017, Fig. 6) and Pinheiro and Rodrigues (2017, Fig. 2J), including: (G), cf. *Lonchodraco* sp.; (H) *Azhdarcho lancicollis*; (I), *Santanadactylus pricei*; (J), "*A. araripensis*"; (K), *S. spixi*; (L), *Pteranodon* sp.; (M), "*A. santanae*"; (N), *Anhanguera piscator*, (O) *Anhanguera* sp. AMNH 22555, and (P), cf. *Anhanguera*. **Abbreviations**: **cr,** crest; **dar,** articulation surface for radius; **dau,** articulation surface for ulna; **fov,** fovea; **ftp,** flexor tendon process; **isa,** intersyncarpal surface articulation; **pf,** pneumatic foramen; **sul,** sulcus; **tu,** tuberosities. Black arrows indicate pneumatic foramina in (C) to (F). Scale bar equals 2 cm.

slightly more than half its transverse width. The distal articular surface is slightly expanded dorsally and developed into an elongate articular surface exposed on the posterior and distal faces of the element. This articular surface also has a very small excursion onto the anterior face of the element, where it is positioned just below a prominent tubercle. On the opposite side of the anterior face lies a prominent crest that is oriented parallel to the long axis of the bone. In distal view, the articular surface of the radius is roughly peanut-shaped, with a larger dorsal articular surface and a much smaller ventral articular surface. The anterior suface of the bone bears striated marks that we interpret to be muscle attachment scars.

A transverse histological section through a small shaft section of the radius exhibits a thin cortex composed of fibrolamellar bone with abundant and small in diameter vascular canals, very few primary osteons, a well-defined endosteal bone layer (Fig. 5D–F). There are no lines of arrested growth. These features are consistent with rapid growth of a sub-adult individual (Ricqlès et al., 2000). The endosteal bone layer is characterized by highly elongated and abundant osteocytes (Fig. 5F), similar to the same bone tissue of *Rhamphorhynchus* from the Solnhofen Limestones (Prondvai et al., 2012). Specimen UR-CP-0233 exhibits some erosional cavities in the posterior bone layer (Fig. 5D–G), which seem to be associated with the origin of the bone struts (Prondvai et al., 2012) that characterize the uncompacted cancellous bone (spongiosa) inner tissue region of the bone. Another pterosaur characteristic visible in

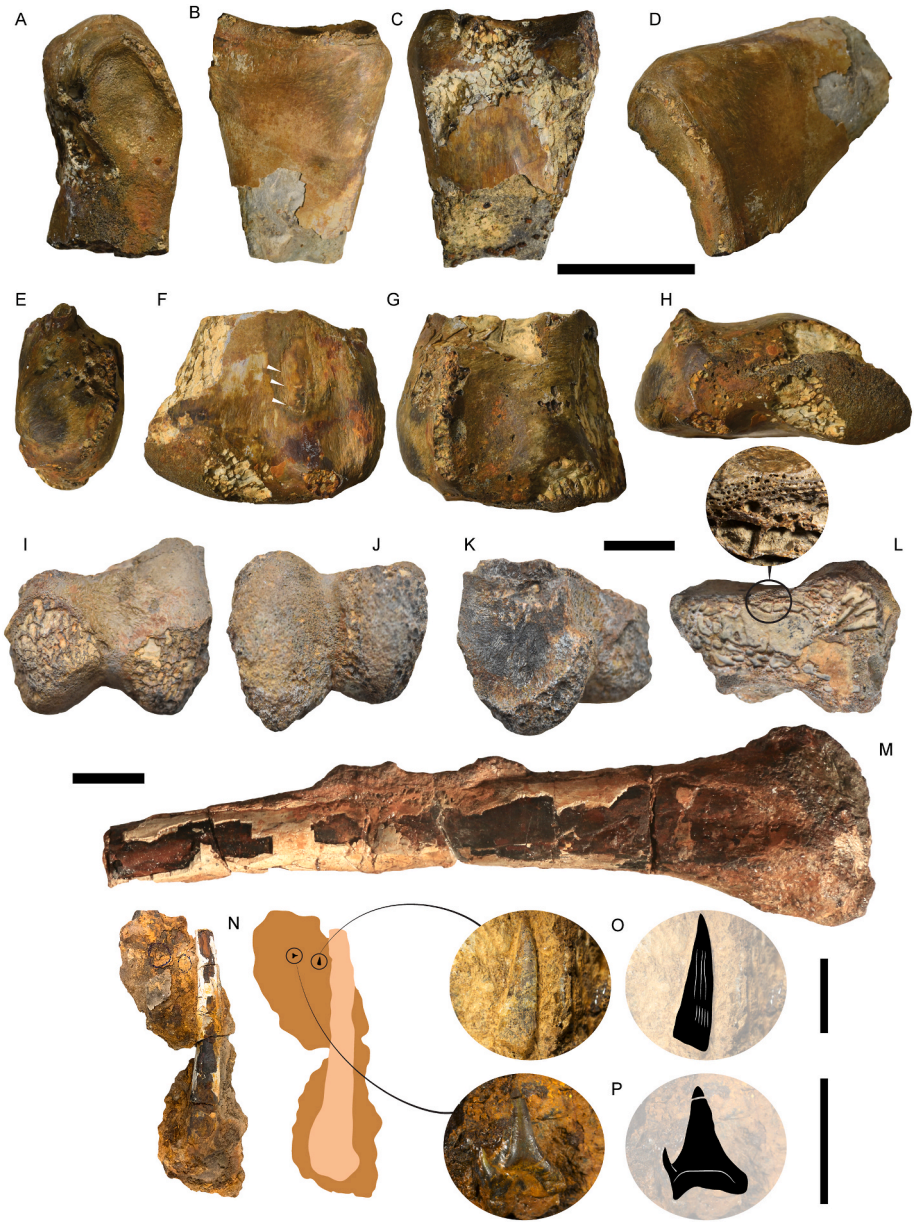

Fig. 4. Specimen UR-CP-0233, UR-CP-0230, and UR-CP-0234. **A–D**, specimen UR-CP-0233, proximal portion of a left radius in: (A) ventral view; (B), anterior view; (C), posterior view; (D) anterodorsal view. **E–H**, specimen UR-CP-0233, distal portion of a left radius in: (E) medial view; (F), anterior view; (G), posterior view; (H) distal view. **I–L**, Anhangueria indet. UR-CP-0230, UR-a distal end of a right metacarpal IV in: (I) posterior view; (J), distal view; (K), distoventral view; (L) in transversal cross section showing the trabecular tissue near the exterior region and more spongy bone at the inner part of the bone. **M–P**, Anhangueria indet. UR-CP-0234, to a left radius with an isolated pterosaur and an isolated shark tooth: (M), left radius in anterior view; (N) left radius before being removed from the rock matrix, indicating where the pterosaur tooth (O) and shark tooth (P) possibly belonging to an odontaspidid were located. Horizontal scale bars equal 2 cm, upper bar applies for (A) to (D), middle bar applies for (E) to (H) and lower bar applies for (N). Vertical scale bars equal 5 mm and apply for (O) and (P) respectively. White arrows in (F) indicate scars for the attachments of muscles.

UR-CP-0233 is the occurrence of periosteal tissue exhibiting 'plywood-like' pattern (Fig. 5H, I, J), which occurs when bone fiber, lacunae, and vascular canals in each lamella have a preferred orientation, creating zonal extinction under polarized-light (Steel, 2008). Remains of 'plywood-like' bone tissue are also observed in some of the struts that form the uncompacted cancellous bone (Fig. 5K and L).

Specimen UR-CP-0233 includes a complete left distal syncarpal element (Fig. 3A–F, O). The bone is very well preserved, with only a very small amount of surface damage to some of the sharp edges on its proximal and distal surfaces. The distal syncarpal is roughly trapezoidal in proximal or distal views. It measures approximately 5 cm wide transversely by 4 cm deep dorsoventrally by 2 cm thick proximodistally.

The proximal surface of the distal syncarpal is topographically complex. It is predominated by two subtriangular projections, the intersyncarpal articular surfaces, that are separated from one another by a deep, obliquely oriented sulcus that extends from the dorsolateral to the ventromedial corner of the element. Small foramina open in the dorsomedial portion of the sulcus; the largest of these faces laterally. The intersyncarpal articular surfaces are subtriangular in shape and inverted relative to one another, with their hypotenuses bordering the sulcus. The dorsal intersyncarpal articular surface is larger, more extensive dorsoventrally, and slightly more expanded proximally. By contrast, the

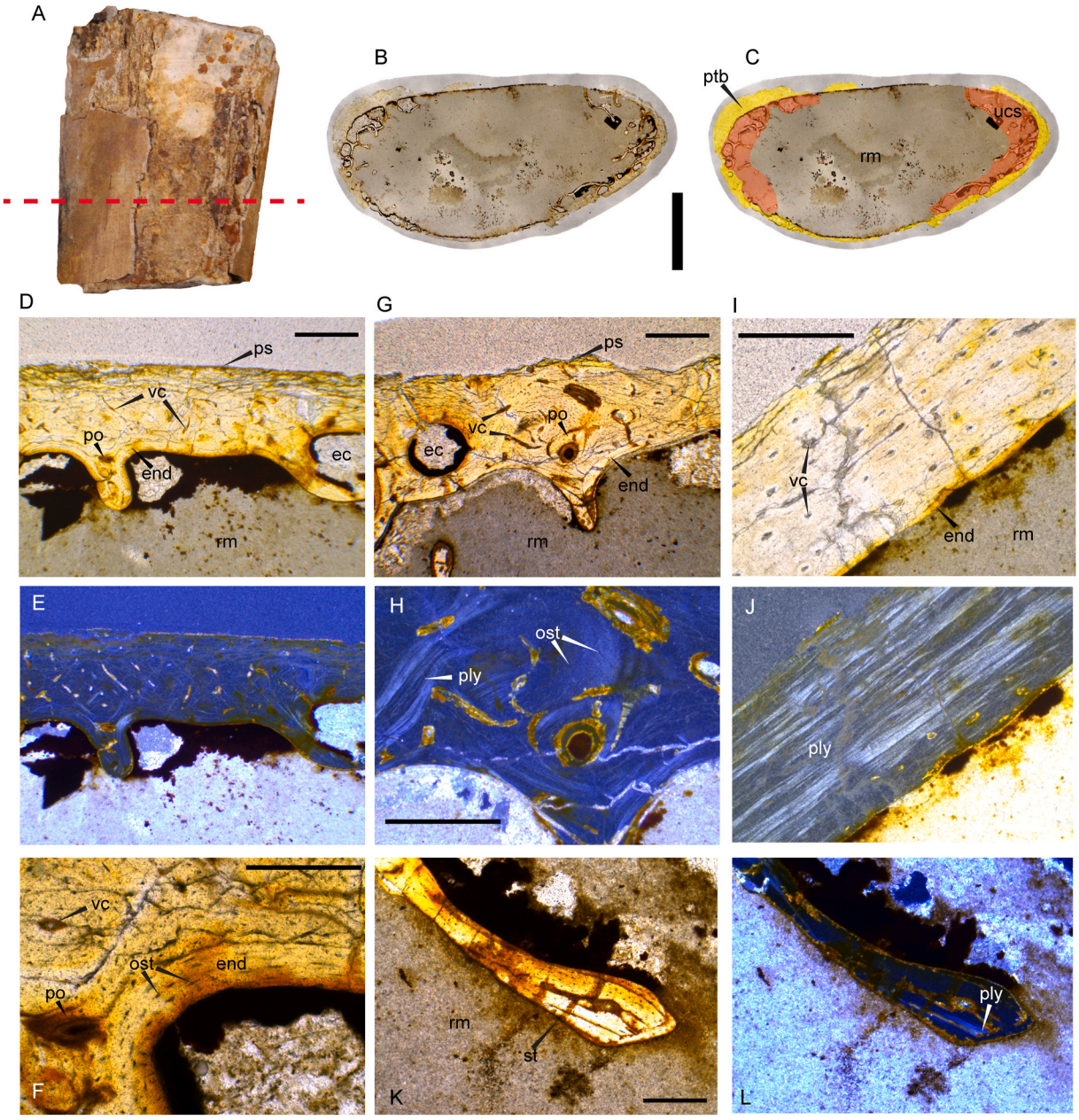

Fig. 5. Bone histology of a shaft radius fragment of specimen UR-CP-0233. **A**, the bone fragment in anterior view, indicating where the thin section was elaborated (red dotted line); **B–C**, full view of the bone thin section showing where the different tissue types are preserved versus the infilling rock matrix; **D–J**, transverse section of three different regions of periosteal bone: in transmitted light (TL) (D) region 1, (G) region 2, (I) region 3 and (F) zoom-up of the endosteal internal layer of region 1; in crossed polarized with DLF filter (PL-DLF) (E) region 1, (H) zoom of the middle part of region 2, and (J) region 3 in crossed polarized; **K–L**, transverse section of a strut of the uncompacted cancellous bone (spongiosa) region in TL (K) and PL-DLF (L). **Abbreviations**: **ec,** erosion cavity; **end,** endosteal lamellar bone; **ost,** osteocyte-lacuna; **ply,** 'plywood' layers; **po,** primary osteon; **ps,** periosteal bone surface; **pts,** periosteal-trabecular bone; **rm,** rock matrix; **st,** strut; **ucs,** uncompacted cancellous bone (spongiosa); **vc,** vascular canal. Upper vertical scale bar equals 1 cm, and scale bars included in the microphotographs equals 500 μm [planned for page width].

ventral intersyncarpal articular surface is smaller, more restricted dorsoventrally, and less expanded proximally. The highest points of both intersyncarpal articular surfaces are near the lateral margin of the distal syncarpal. On the opposite side of the same face, the ventromedial corner comes to a blunted point that represents the articular surface for the medial ("preaxial") carpal.

The distal surface of the distal syncarpal has less topographical relief than does the proximal surface, but it is more complex morphologically. It bears a prominent fovea that is approximately 1 cm in diameter by 1 cm deep and positioned slightly medial to the geometric center of the element. The fovea appears to be pneumatic, with smaller pneumatic foramina opening within it. It is partially ringed by a flattened crest that is approximately 0.5 cm broad. There is a gap in the crest on the dorsomedial margin of the fovea, from which a gentle groove emanates and extends onto the dorsal surface of the element. The crest separates the fovea from the articular surface for the metacarpus, principally metacarpal IV, which is located on the lateral side of the distal syncarpal. The metacarpal articular surface is reniform in outline and stepped proximodistally. Although the surface is contiguous, the sharp step creates a distinction between dorsal and ventral articular surfaces that can be identified in lateral view of the element. The dorsal metacarpal articular surface is smaller and transversely oriented, whereas the ventral metacarpal articular surface is ear-shaped and dorsoventrally oriented. Two small foramina open near the ventral extreme of the ventral metacarpal articular surface.

The ventral surface of the distal syncarpal bears a relatively large foramen (ca. 0.25 cm diameter) and several much smaller foramina. The dorsal surface of the distal syncarpal is notched medially, marking the position of the gentle groove exiting the fovea.

ANHANGUERIA indet.

(Fig. 4I–O).

Referred material—Two specimens are referred to Anhangueria indet. Specimen UR-CP-0230 is a distal end of a right metacarpal IV, and specimen UR-CP-0234 is a proximal portion of a left radius and an isolated tooth.

Localities, Horizons, and Age—The distal metacarpal IV (UR-CP-0230) is from Pico de la Vieja North locality, which is located approximately 6 km north-northeast of Zapatoca, in the Department of Santander, Colombia (6° 51′ 18'' N, 73° 13′ 51'' W). The specimen was collected from a thick layer of iron-calcareous rich mudstone between R-R′ horizons of the Carrizal Member, Rosa Blanca Formation (Etayo-Serna and Guzmán-Ospitia, 2019). The Rosa Blanca Formation is from the upper Valanginian stage of the Lower Cretaceous.

A proximal radius and isolated tooth (UR-CP-0234) were collected from the El Mirador los Monos locality, which is located approximately 6 km north of Villanueva, in the Department of Santander, Colombia (6° 43′ 32" N, 73° 9′ 48" W). The specimen was collected from the base of La Paja Formation, which has been suggested to correspond to the lower Barremian stage of the Lower Cretaceous (Patarroyo, 2020).

Description—Specimen UR-CP-0234 corresponds to a left radius (Fig. 4M and N). Most of the external bone tissue is eroded, and the hollow internal cavity was in filled by hematite (Fig. 4M). The bone was preserved in a hard rock matrix composed of hematite and gypsum (Fig. 4N). In this rock matrix, we found one isolated tooth exhibiting a sigmoid profile and enamel ornamentation consisting of faint, reticulated, longitudinal ridges (Fig. 4O). Also, very close to this tooth, an isolated shark tooth was also preserved (Fig. 4P).

Specimen UR-CP-0230 is the distal end of a right metacarpal IV (Fig. 4I–L). In posterior and distal views (Fig. 4I and J), it exhibits the two robust distal condyles for the articulation with wing phalanx 1. The bone surface is eroded at both distolateral regions showing tissue with high pneumaticity in posterior view. In distoventral view (Fig. 4K), the metacarpal exhibits a very flat surface and a circular and deep pneumatic foramen. Due to a natural breakage, the trabeculae at the external surface of the bone, and the spongy, highly pneumatic internal bone tissue are visible in cross section (Fig. 4L).

A transverse histological section through the shaft of metacarpal IV (UR-CP-0230; Fig. 6) reveals that the periosteal layer has been replaced almost completely by trabecular bone with large erosional cavities. Lines of arrested growth and well-defined external circumferential lamellae are visible (Fig. 6F and G), indicating an adult individual with periods of interrupted growth and skeletal maturity (Andrade et al., 2015; Kellner et al., 2013; de Ricqlès et al., 2000; Steel, 2008). Similar bone features have been also documented in a pterosaur with anhanguerid affinities from the Aptian Romualdo Formation of Brazil (Bantim et al., 2021). The trabecular tissue varies in thickness along the cross section of the bone, being particularly thick at the posterior and anterior sides (Fig. 6C, D, E), potentially due to difference in load and biomechanical function of the bone. This hypothesis is supported by the occurrence of Sharpey's fibers (Fig. 6H and I), indicating zones for the attachment of tendons and ligaments to the bone. The struts forming the inner uncompacted cancellous bone exhibit some peripheral lamellae and occasional secondary osteons (Fig. 6J and K).

4. Discussion

The partial jaws of specimen UR-CP-0233 (Fig. 2J) resemble those of "*Anhanguera* (*Santanadactylus*) *araripensis*" (Fig. 2K), *A.* (*Maaradactylus*; *Coloborhynchus*) *spielbergi* (Veldmeijer, 2003; Rodrigues and Kellner, 2013), "*A.* (*Araripesaurus*) *santanae*" (Pinheiro and Rodrigues, 2017), and a specimen of *Anhanguera* (Veldmeijer et al., 2005, Fig. 3)—all of which exhibit a large fossa depressoria and moderately long retroarticular process ending in U-shaped margin seen in dorsal view. However, specimen UR-CP-0233 differs from "*A. araripensis*", *A. spielbergi,* "*A. santanae*," and the rami of other pterosaurs figured in Pêgas et al. (2021) in having triangular shape of the glenoid fossa in dorsal view, a fossa depressoria exhibiting a bean-shaped outline, and a retroarticular process that exhibits a straight margin in lateral or medial views. The rami of other pterosaurs differ more notably from specimen UR-CP-0233. For example, in *Pteranodon* sp. YPM- 2410 (Fig. 2L), the retroarticular process is longer and narrower, the fossa depressoria elongated in shape, and the glenoid fossa larger forming a trapezoidal shape in dorsal view. In the *Thalassodromeus sethi* holotype (Fig. 2M), the retroarticular process is shorter, and the fossa depressoria exhibits a circular outline. In the *Aymberedactylus cearensis* holotype (Fig. 2N) the rami are very narrow, as is the retroarticular process, and in *Pteranodon* sp. LACM- 51130 (Fig. 2O) the fossa depressoria is small and the glenoid fossa wider. The bone surface striations and rod-like shape of the ceratobranchial bone of specimen UR-CP-0233 (Fig. 2P–R) ressemble several other pterosaurs (Jiang et al., 2020; Fig. 3), in particular *Nurhachius ignaciobritoi*.

The distal syncarpal of specimen UR-CP-0233 (Fig. 3A–F, O) differs in terms of its shape, fovea, and articular facets for the ulna and radius compared to the same bone of Cretaceous pterodactyloids figured in Rigal et al. (2017, Fig. 3) including: cf. *Lonchodraco* sp. (Fig. 3G); *Azhdarcho lancicollis* (Fig. 3H); *Santanadactylus pricei* (Fig. 3I); "*A. araripensis*" (Fig. 3J); *S. spixi* (Fig. 3K); *Pteranodon* sp. (Fig. 3L); "*A. santanae*" (Fig. 3M); *Anhanguera piscator* (Fig. 3N). It also differs from the narrower syncarpal of *A. spielbergi* (Veldmeijer, 2003) and that of *Ferrodraco lentoni* (Pentland et al., 2022). The distal syncarpal of specimen UR-CP-0233 is similar in general shape and proportions of the fovea, facets, and foramina to the syncarpal of *Anhanguera* sp. (AMNH 22555; Pinheiro and Rodrigues, 2017, Fig. 3P). The similarity between these specimens supports the attribution of UR-CP-0233 to Anhangueria.

The isolated tooth of UR-CP-0234 (Fig. 4O) from La Paja Formation resembles the labiolingual compression, sigmoid profile, slight distal curvature, and enamel ornamentation of longitudinal grooves exhibited by other members of Ornithocheiridae or Anhangueria/Anhangueridae, as does a recent tooth described from the Early Cretaceous of Ukraine (Brougham et al., 2017; Sokolskyi, 2023). The shark tooth (Fig. 4P) preserved in proximity to the pterosaur tooth and radius of UR-CP-0234 reseembles teeth from odontaspidid sharks, particularly of

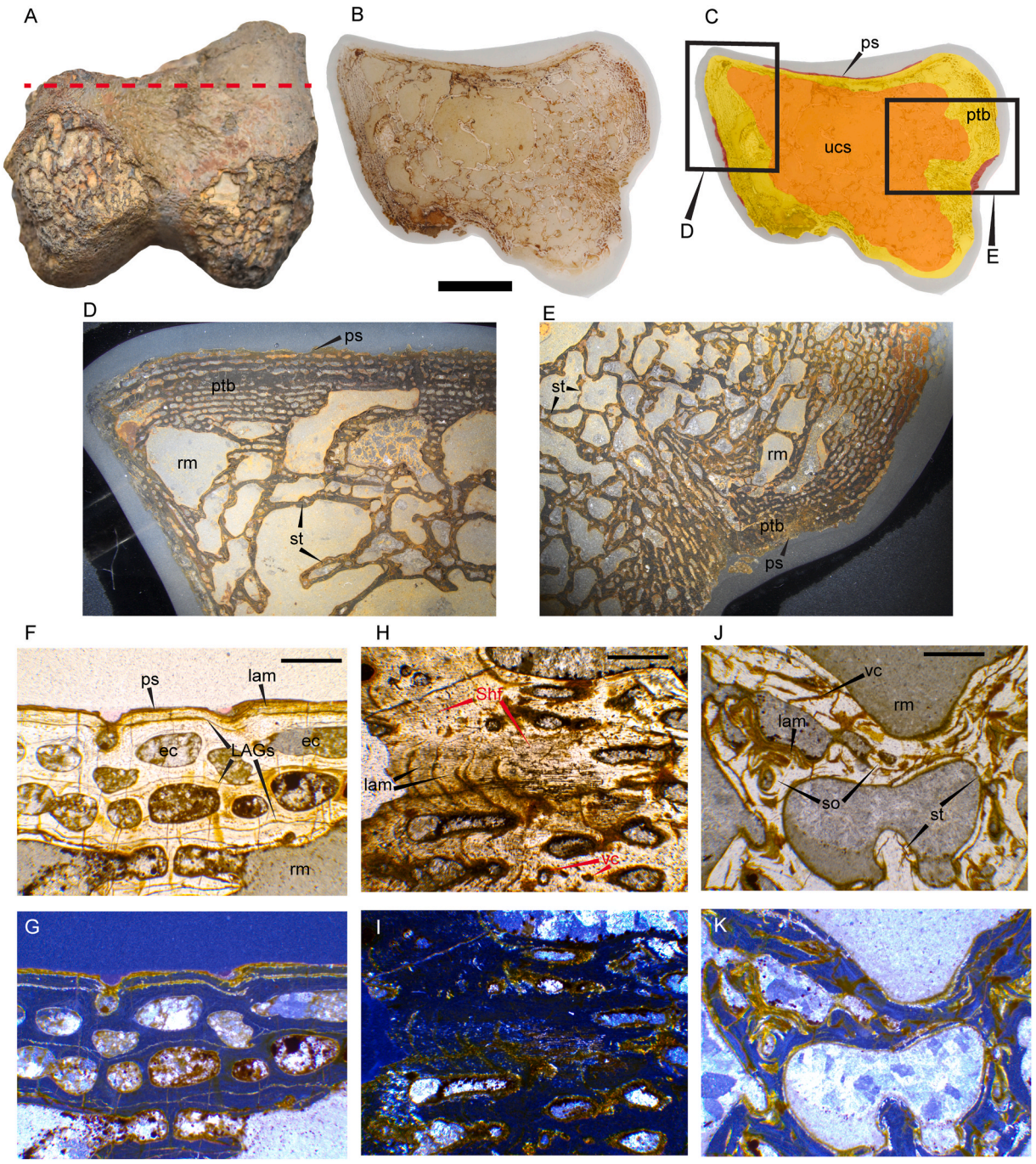

Fig. 6. Bone histology of Anhangueria indet. UR-CP-0230 distal end of a right metacarpal IV. **A**, the bone fragment in posterior view, indicating where the thin section was elaborated (red dotted line); **B–C**, full view of the bone thin section showing where the different tissue types are preserved versus the infilling rock matrix; **D–E**, close-ups of two regions of the thin section showing in detail the tissue types, see rectangles showed in (D); **D–J**, transverse section of two different regions of periosteal bone: in transmitted light (TL) (F) region 1, (H) region 2, in crossed polarized with DLF filter (PL-DLF) (G) region 1, (I) region 2; **J–K**, transverse section of the uncompacted cancellous bone (spongiosa) region in TL (J) and PL-DLF (K). **Abbreviations**: **ec,** erosion cavity; **LAG**, line of arrested growth; **lam,** lamellar bone; **ps,** periosteal bone surface; **pts,** periosteal-trabecular bone; **rm,** rock matrix; **Shf,** Sharpey fiber; **so,** secondary osteon; **st,** strut; **ucs,** uncompacted cancellous bone (spongiosa); **vc,** vascular canal. Upper vertical scale bar equals 1 cm, and scale bars included in the microphotographs equals 500 μm.

Eostriatolamia (Glickman and Averianov, 1998). This suggests a thanatocoenosis assemblage type, where marine sharks and flying pterosaurs were buried and preserved together. A similar thanatocoenosis assemblage occurs with the pterosaurs of the Rosa Blanca Formation, which are usually found together with marine invertebrates and pycnodontiform fish remains.

5. Conclusions

The fossil pterosaurs from Colombia described herein expand our understanding of the pterosaur diversity of northern South America during the Early Cretaceous. The fossils include a new record of Anhangueridae—based on mandibular remains, a ceratobranchial bone, a distal syncarpal, and portions of a radius—that may constitute a distinct taxon. Additional fossil remains referrable to the more inclusive

group Anhangueria include a partial metacarpal IV and an isolated partial radius. Histological analysis of two bones provides some insights into the growth patterns of these pterosaurs. Based on this analysis, specimen UR-CP-0233 represents a juvenile individual and specimen UR-CP-0230 an adult, both sharing with other fossil pterosaurs bone tissues that indicate rapid growth. These new pterosaur fossils from the Valanginian and Barremian of Colombia show that these flying reptiles were well adapted to inhabit the coastal conditions prevailing during that time in northern South America. This is also supported by the occurrence of juveniles and adults, potentially giant, larger than 5 m long wingspan. Further studies and exploration in this area could potentially uncover more fossils and enrich our knowledge of pterosaur biology and paleontology in the region.

CRediT authorship contribution statement

Edwin-Alberto Cadena: Writing – review & editing, Writing – original draft, Visualization, Validation, Supervision, Resources, Project administration, Methodology, Investigation, Funding acquisition, Formal analysis, Data curation, Conceptualization. **Dubban A. Atuesta-Ortiz:** Investigation, Formal analysis. **Jeffrey A. Wilson Mantilla:** Writing – review & editing, Writing – original draft, Methodology, Investigation, Formal analysis.

Declaration of competing interest

The authors declare that they have no known competing financial interests or personal relationships that could have appeared to influence the work reported in this paper.

Acknowledgements

We thank to J. Parra and F. Parra from the Centro de Investigaciones Paleontológicas, Villa de Leyva, Colombia, for helping with the preparation of specimen UR-CP-0234. This research was supported by the Dirección de Investigaciones e Innovación, Universidad del Rosario, Proyectos de Investigación (grant IV-FMD001, 2022 to E-A. C.)

Data availability

Data will be made available on request.

References

Andrade, R.C.L.P., Bantim, R.A.M., Lima, F.J., Campos, L.S., Eleuterio, L.H.S., Manso-Sayão, J.M., 2015. New data about the presence and absence of the external fundamental system in archosaurs. Cadernos de Cultura e Ciência. 14, 200–211.

Andres, B., Langston, W., 2021. Morphology and taxonomy of *quetzalcoatlus* lawson 1975 (pterodactyloidea: azhdarchoidea). In: Padian, K., Brown, M.A. (Eds.), The Late Cretaceous Pterosaur *Quetzalcoatlus* Lawson 1975 (Pterodactyloidea: Azhdarchoidea), pp. 46–202. Society of Vertebrate Paleontology Memoir 19 Journal of Vertebrate Paleontology, 41(sup.1.

Bantim, R.A.M., Andrade, R.C.L.P., Sobreira-Ferreira, J., Feitosa-Saraiva, A.A., Kellner, A.W.A., Manso-Sayão, J., 2021. Osteohistology and growth pattern of a large pterosaur from the lower cretaceous Romualdo Formation of the araripe basin, northeastern Brazil. Cretac. Res. 118, 104667.

Brougham, T., Smith, E.T., Bell, P.R., 2017. Isolated teeth of Anhangueria (pterosauria: pterodactyloidea) from the lower cretaceous of lightning ridge, new South wales, Australia. PeerJ 5, e3256.

Cadena, E.-A., Unwin, D., Martill, D.M., 2020. Early cretaceous pterosaurs from Colombia. Cretac. Res. 114, 104526.

Campos, D.A., Kellner, A.W.A., 1985. Panorama of the flying reptiles study in Brazil and South America. An Acad. Bras Ciências 57, 453–466.

de Ricqlès, A., Padian, K., Horner, J.R., Francillon-Viellot, H., 2000. Paleohistology of the bones of pterosaurs (Reptilia: archosauria): anatomy, ontogeny and biochemical implications. Zool. J. Linn. Soc. 129, 349–385.

Etayo-Serna, F., Guzmán-Ospitia, G., 2019. Formación Rosa Blanca: subdivisión de la Formación y propuesta de neoestratotipo. Sección laguna El Sapo, vereda El Carrizal, Municipio de Zapatoca, Departamento de Santander. In: Etayo-Serna, F. (Ed.), Estudios Geológicos y Paleontológicos Sobre el Cretácico en la Región del Embalse del Río Sogamoso, Valle Medio del Magdalena. Compilación de los Estudios Geológicos Oficiales en Colombia XXIII. Servicio Geológico Colombiano, Bogotá, pp. 3–54.

Glickman, L.S., Averianov, A.O., 1998. Evolution of the Cretaceous lamnoid sharks of the genus *Eostriatolamia*. Paleontol. J. 32, 376–384.

Jiang, S., Li, Z., Cheng, X., Wang, X., 2020. The first pterosaur basihyal, shedding light on the evolution and function of pterosaur hyoid apparatuses. PeerJ 8, e8292.

Kaup, J.J., 1834. Versuch einer Eintheilung der Saugethiere in 6 Stämme und der Amphibien in 6 Ordnungen. Isis von Oken 3, 311–324.

Kellner, A.W., Campos, D.A., Sayão, J.M., Saraiva, A.A, Rodrigues, T., Oliveira, G., Cruz, L.A., Costa, F.R., Silva, H.P., Ferreira, J.S., 2013. The largest flying reptile from Gondwana: a new specimen of *Tropeognathus* cf. T. *mesembrinus* Wellnhofer, 1987 (Pterodactyloidea, Anhangueridae) and other large pterosaurs from the Romualdo Formation, Lower Cretaceous, Brazil. An. Acad. Bras. Cienc. 85 (1), 113–135.

Kellner, A.W.A., Moody, J.M., 2003. Pterosaur (Pteranodontoidea, Pterodactyloidea) Scapulocoracoid from the Early Cretaceous of Venezuela, vol. 217. Geological Society, London, Special Publication, pp. 73–77.

Patarroyo, P., 2020. Barremian deposits of Colombia: a special emphasis on marine successions. In: Gómez, J., Pinilla-Pachón, A.O. (Eds.), The Geology of Colombia, Volume 2 Mesozoic. Servicio Geológico Colombiano, Publicaciones Geológicas Especiales 36, pp. 403–439. Bogotá.

Pêgas, R.V., Costa, F.R., Kellner, A.W.A., 2021. Reconstruction of the adductor chamber and predicted bite force in pterodactyloids (Pterosauria). Zool. J. Linn. Soc. 193, 602–635.

Pentland, A.H., Poropat, S.F., White, M.A., Rigby, S.L., Bevitt, J.J., Duncan, R.J., Sloan, T., Elliott, R.A., Elliott, H.A., Elliott, J.A., Elliott, D.A., 2022. The osteology of *Ferrodraco lentoni*, an anhanguerid pterosaur from the mid-Cretaceous of Australia. J. Vertebr. Paleontol., e2038182

Pinheiro, F.L., Rodrigues, T., 2017. *Anhanguera* taxonomy revisited: is our understanding of Santana Group pterosaur diversity biased by poor biological and stratigraphic control? PeerJ 5, e3285.

Plieninger, F., 1901. Beiträge zur Kenntnis der Flugsaurier. Palaeontographica 48, 65–90.

Prondvai, E., Stein, K., Ösi, A., Sander, P.M., 2012. Life history of *Rhamphorhynchus* inferred from bone histology and the diversity of pterosaurian growth strategies. PLoS One 7, e31392.

Rigal, S., Martill, D.M., Sweetman, S.C., 2017. A new pterosaur specimen from the upper tunbridge wells sand formation (cretaceous, valanginian) of southern england and a review of *Lonchodectes sagittirostris* (owen 1874). In: Hone, D.W.E., Witton, M.P., Martill, D.M. (Eds.), New Perspectives on Pterosaur Palaeobiology. Geological Society, London, Special Publications, pp. 221–232.

Rodrigues, T., Kellner, A.W.A., 2013. Taxonomic review of the *ornithocheirus* complex (pterosauria) from the cretaceous of england. ZooKeys 308, 1–112.

Rosenbach, K.L., Goodvin, D.M., Albshysh, M.G., Azzam, H.A., Smadi, A.A., Mustafa, H. A., Zalmout, I.S., Wilson-Mantilla, J.A., 2024. New pterosaur remains from the Late Cretaceous of Afro-Arabia provide insight into flight capacity of large pterosaurs. J. Vertebr. Paleontol., e2385068

Seeley, H.G., 1870. T. He Ornithosauria: an Elementary Study of the Bones of Pterodactyls, Made from Fossil Remains Found in the Cambridge Upper Greensand, and Arranged in the Woodwardian Museum of the University of Cambridge. Bell, and Co., Deighton, p. 135. Cambridge, xii.

Sokolskyi, T., 2023. First occurrence of pterosaurs in Ukraine from the albian (lower cretaceous) burim formation, kaniv natural reserve. J. Vertebr. Paleontol. 43, e2238000.

Steel, L., 2008. The palaeohistology of pterosaur bone: an overview. In: E Buffetaut, E., Hone, D.W.E. (Eds.), Flugsaurier: Pterosaur Papers in Honour of Peter Wellnhofer. Zitteliana, Series B, vol. 28, pp. 109–125.

Szives, O., Moreno-Bedmar, J.A., Aguirre-Urreta, B., Company, M., Frau, C., López-Horgue, M., Pictet, A., Ploch, I., Salazar, C., Barragán, R., Latil, J.-L., Lehmann, J., Robert, E., Reboulet, S., 2024. Report on the 7th international meeting of the IUGS lower cretaceous ammonite working group, the kilian group (warsaw, Poland, 21st august 2022): state of the art on the current standard ammonite zonation of the western tethyan mediterranean province. Cretac. Res. 153, 1–14.

Veldmeijer, A.L., 2003. Description of *Coloborhynchus spielbergi* sp. nov. (Pterodactyloidea) from the albian (lower cretaceous) of Brazil. Scripta Geol. 125, 35–139.

Veldmeijer, A.J., Signore, M., Meijer, H.J.M., 2005. Description of two pterosaur (pterodactyloidea) mandibles from the lower cretaceous santana formation, Brazil. Deinsea 11, 67–86.